ANALYSIS OF THE CAUSE OF THE FRACTURE OF THE PISTON ROD OF THE SPILLWAY FLOODGATE OF TUCURUÍ HYDROELECTRIC POWER PLANT

Davi Carvalho Moreira

davicarvalhomoreira@hotmail.com.br

Centrais Elétricas do Norte do Brasil S/A

Rod. BR 422 Km 13 UHE Tucuruí, CEP 68464-000, Tucuruí, Pará, Brazil

Bruno Merlin

Rafael Araújo de Sousa

Luís Augusto Conte Mendes Veloso

Debora Dias Costa Moreira

bruno.merlin@gmail.com

rfldesousa@hotmail.com

ticoveloso@uol.com.br

deborinhadias@hotmail.com

Federal Univeristy of Pará

Rod. BR 422 Km 13 UFPA, CEP 68464-000, Tucuruí, Pará, Brazil

Abstract: *This paper presents a technical investigation that analyzes the cause of the fracture in some movement piston rods of the spillway floodgates of Tucuruí hydroelectric power plant. This investigation was divided into two parts: experimental and theoretical. Structural elements were monitored in a real service situation, with forces measured by strain gages. The results obtained in the experimental test were used in numerical solutions based on the Finite Element Method to check stress concentrations present in the notch of the piston rod, performing a fatigue analysis by the* ε*-N method of crack initiation and analyzing different semi-elliptical cracks to identify the approximate size that causes the rupture of the piston rod.*

Keywords: *Crack, Fatigue, Piston rod, Spillway.*

1 INTRODUCTION

Tucuruí Hydroelectric power plant (HPP Tucuruí) has one of the biggest spillways in the world with a total capacity of 110,000 m^3/s, as shown in Fig. 1. The main function of the spillway is to release all the exceeding water, not used for energy generation, keeping the reservoir level within the normal operation range, and preserving the stability of the slopes of the reservoir banks. The spillway of Tucuruí is built to face an exceptional flood with an occurrence probability of 1/1000 years. During the 35 years of Tucuruí dam existence, the greatest flow rate registered in the spillway was 68,400 m^3/s, which is about 62% of the maximum capacity. Tucuruí's spillway has 23 floodgates, with individual flow capacity of 4,780 m^3/s. Two hydraulic cylinders enable to open and close a floodgate. The piston rods and cylinders were designed to work during the whole dam life. However, cracks and ruptures have begun to appear in several piston rods.

Figure 1. Spillway of HPP Tucuruí

Beyond the financial loss, the rupture of one of the piston rods makes the floodgate unusable. It consequently reduces the flow capacity of the spillway and may cause a security problem in the dam. Besides that, disabling o floodgate affects the structural behavior of the neighboring floodgates. In fact, for structural reasons, neighboring floodgates shall not release very different water outflows. As a consequence, disabling a floodgate may reduce more than 15% of the spillway capacity instead of 4.3% (corresponding to the full capacity of a floodgate). During the years of operation, three piston rods fractured and eight cracks were detected in piston rods of different floodgates, as presented in Table 1.

Table 1. Sequential of Events of the Fractures and Cracks in Piston Rods

Event	Description	Period
#1	Fracture in Piston Rod Nº 30 (Floodgate 15)	June/1995
#2	Crack in Piston Rods Nº 3, 10, 12, 14, 15, 18, 24, 32, 34	October/1997
#3	Fracture in Piston Rod Nº 3 (Floodgate 2)	January/2013
#4	Fracture in Piston Rod Nº 37 (Floodgate 19)	February/2015

From a three-dimensional numerical analysis based on the Finite Element Model (FEM), this paper analyzes the structural behavior of the piston rods operating at the spillway floodgates in Tucuruí. The ε-N method is used to detect the crack initiation time. Besides that, different sizes of semi-elliptical cracks are simulated to determine the approximate size that may cause the piston rod rupture.

The methodology consisted in (i) measuring the stresses and strains occurring at the end of the piston rod in a real operational situation; (ii) creating a 3D geometry of the end of the piston rod for a FEM analysis; (iii) doing a fatigue analysis, performing a cyclic work simulation using forces and frequencies resulting from the measurement in real conditions; (iv) analyzing different cracks to understand the rupture contexts.

At first, a test in true operational conditions was performed, consisting of measuring strains in the piston rod in order to calculate the stresses acting on it during floodgate opening and closure. All measurements were taken with the floodgate opened, i.e., the water flow was considered.

Rosette and unidirectional strain gages were installed at the largest diameter section of the piston rod, close to where cracks are appearing. It was not possible to access the smallest diameter section of the piston rod, where the crack occurs, because it is located inside its bottom fork clevis. The stress values where the cracks occur were obtained in the simulations. During the floodgate opening, the mean stress measured at the piston rod was in accordance to what was designed. During its closure, it was observed in one of the piston rods a stress due to unexpected flexure. Friction at the bottom fork clevis bearing increased 19.0 MPa on the stress measured by the rosette strain gages. With the floodgate opened and a constant water flow, a mean tensile stress of 67.22 MPa was measured in the longitudinal direction of the piston rod, with a variation of about 0.2 MPa and a frequency of about 2.8 Hz.

The second step of this study consisted in generating a 3D model that represents the threaded end of the piston rod. In this context, it was used a commercial software (ANSYS) to model the object, create a finite element mesh and calculate the results. All construction details of the piston rod were inserted, such as the screw thread, bevels and notches. The notch with the highest stress concentration of the piston rod had a local control of the mesh to generate better results.

Simulations were performed using ε-N method, based on (i) operational condition measures toward frequency and stresses amplitude variation, caused by the water flow through the floodgate, (ii) estimation of the ε-N method constants for the piston rod steel. The simulations are supposed to estimate the piston rod lifespan before crack appearance due to fatigue. The movement piston rods of the spillway floodgate are made of martensitic stainless steel, specified by ASTM A 276 as type 410 (or AISI 410) T-property. This property means that the steel is hardened by heat and other thermic treatments at a relative high temperature. For the simulation, the aforementioned standard values were used, to estimate the parameters related to fatigue and the load was modeled by a sinusoid, with data collected during field test.

In relation to simulation results, an analysis of the convergence and quality of the software mesh was performed. It was observed that the region with the highest stress concentration is the smallest diameter section of the piston rod, close to the notch, where cracks and fractures are occurring.

To finalize the study, different semi-elliptical cracks generated during the simulation were analyzed. During this analysis, for the ASISI 410 steel, it was considered the critical tenacity value of a stress intensity factor (K_{IC}), frequently used in the literature (1,319 MPa $\sqrt{mm}$). Then, an equivalent estimation for the *J integral* to analyze the tenacity at the fracture was obtained. The plastic zones generated at the crack end were analyzed by von Mises stresses. The crack study presented approximate sizes of cracks that exceed the critical value from the *J integral* and, hence, would generate the piston rod rupture.

As a result, the fatigue studies indicate it is unlikely that the appearance of cracks in the piston rod occurs exclusively due to water flow through the floodgate, because the amplitude of stress variation is very low. Friction at the bottom fork clevis bearing, probably due to lack of lubrification, causes an increase in the notch of the piston rod stresses that accelerates the propagation of an existing crack.

The fatigue studies also conducted to an investigation of the spare rods, which is performed from a metallographic replic test. This procedure is done to detect surface cracks. Studying a crack propagation method to estimate the rupture occurance time of the piston rod will be a continuation of this research.

This paper provides important information for including fatigue studies in the specification of future piston rods of the spillway floodgate of HPP Tucuruí and other spillways. As a byproduct, this paper also intends to provide recommendations about the maintenance procedure that will help enhancing the lifespan of the piston rod and perform preventive replacement of the damaged piston rods. Finally, the study will help maintaining the spillways of Tucuruí to their maximum capacity and preserve the safety of the dam.

2 BIBLIOGRAPHIC REVIEW

FEM is a widely used tool to determine the structural behavior of components when subjected to static and/or dynamic loads.

2.1 Fatigue

In a study performed by Melo et al. (2005), finite element technics of detecting and eliminating chronic structural problems in devices subjected to cyclic loads were used. With the model calibration, it was possible to perform a complete analysis to fatigue in critical regions, allowing to check the best solution for structural problems of the device.

In this paper, the ε-N method developed by Coffin and Manson to analyze fatigue is used, because its analysis base is the material strain (elastic and plastic). This phenomenon is typically divided into two parts (elastic and plastic) (Chaves, 2010):

$$\frac{\Delta\varepsilon}{2} = \frac{\Delta\varepsilon_{el}}{2} + \frac{\Delta\varepsilon_{pl}}{2} \tag{1}$$

where,

$$\frac{\Delta\varepsilon}{2} = Total\ strain$$

$$\frac{\Delta\varepsilon_{el}}{2} = Elastic\ strain$$

$$\frac{\Delta\varepsilon_{pl}}{2} = Plastic\ strain$$

The ε-N method uses real stresses and strains, modelling the elastoplastic hysteresis loops by a single Ramberg-Osgood relation and assumes that a single equation describes all hysteresis loops:

$$\frac{\Delta\varepsilon}{2} = \frac{\Delta\sigma}{2E} + \left(\frac{\Delta\sigma}{2H_c}\right)^{\frac{1}{h_c}} \tag{2}$$

where,

$$\Delta\sigma = Variation\ of\ the\ notch\ Stress$$

$$H_c = Coefficient\ of\ Cyclic\ Tightening$$

$$h_c = Exponent\ of\ Cyclic\ Tightening$$

$$E = Modulus\ of\ Elasticity$$

Assuming that the nominal stresses $\Delta\sigma_n$ are elastic, the Neuber rule can be used in the ε-N method, to model the concentration of stresses and strains in the notches.

$$K_t^2 = \frac{\Delta\sigma\ \Delta\varepsilon\ E}{\Delta\sigma_n^2} \tag{3}$$

where,

$$K_t = Factor\ of\ Stress\ Concentration$$

$$\Delta\sigma_n = Variation\ of\ the\ Nominal\ Stress$$

In the development of ε-N methodology by Coffin and Manson the following relation was obtained:

$$\frac{\Delta\varepsilon}{2} = \frac{\sigma_c}{E}(2N)^b + \varepsilon_c(2N)^c \quad (4)$$

where,

$2N = Number\ of\ Stress\ Reversals\ until\ failure$

$\sigma_c = Coefficient\ of\ Fatigue\ Resistance$

$b = Exponent\ of\ Fatigue\ Resistance$

$\varepsilon_c = Coefficient\ of\ Fatigue\ Ductibility$

$c = Exponent\ of\ Fatigue\ Ductibility$

The coefficient of fatigue resistance (σ_c) and the exponent of fatigue resistance (b) of the elastic part, as well as the coefficient of fatigue ductility (ε_c) and the exponent of fatigue ductility (c) of the plastic part from Coffin-Manson curve are parameters of the ε-N Coffin-Manson curve. In this paper, the base was the Estimates by Medians (Meggiolaro and Castro, 2002), as presented in Table 2, because according to Meggiolaro and Castro (2004) the estimates of the medians are the best ones to estimate the mentioned parameters.

Table 2. Parameters of the ε-N Coffin-Manson curve by Estimate of the Medians

Material property	Value
Coefficient of fatigue resistance (σ_c)	1035 MPa (1.52*S_R)
Exponent of fatigue resistance (b)	-0.09
Coefficient of fatigue ductility (ε_c)	0.45
Exponent of fatigue ductility (c)	-0.59

Considering the adjustments of elastic and plastic strains of the loops by Ramberg-Osgood and the ε-N curve by Coffin-Manson to be perfect, Eq. (2) and (4) can be used to obtain the following relations:

$$h_c = \frac{b}{c} \quad (5)$$

$$H_c = \frac{\sigma_c}{\varepsilon_c^{h_c}} \quad (6)$$

Using the parameters of Table 2, the coefficient of cyclic tightening (H_c) and the exponent of cyclic tightening (h_c) were calculated and are presented in Table 3.

Table 3. Parameters of the Ramberg-Osgood relation

Material Property	Value
Coefficient of Cyclic Tightening (H_c)	901 MPa
Exponent of Cyclic Tightening (h_c)	0.137

2.2 Fracture Mechanics

According to (Chiodo, 2009), the monoparametric fracture mechanics is based on using a single parameter to describe stresses and strains conditions at the end of a crack, and hence evaluate this effect on the integrity of the part.

To evaluate the integrity of the part, by fracture mechanics, tenacity becomes important, because it is a material property that measures the energy the part absorbs before and during the fracture process. The material tenacity makes it resist to a stress field at the end of the crack, without fracturing.

Another important material property, in fracture mechanics, is the tenacity to fracture, that represents the critical value of tenacity for fracturing the part.

In this paper, the used parameters of evaluating tenacity to fracture will be the factor of stress intensity (K) and the *J integral*, on tensile crack opening mode (I). The critical tenacity value for the factor of stress intensity, will be called K_{IC} and for the *J integral*, will be called J_{IC}.

In the study (Hise, 1987), AISI 410 steel has a K_{IC} value of 1,391 MPa$\sqrt{mm}$ at 25ºC. As described in (Srinivasan and Seetharamu, 2012), by Eq. (7), an equivalent value can be obtained to analyze the material tenacity to fracture by *J integral*. For this study, J_{IC} value is 8.8 mJ/mm^2.

$$J_{IC} = \frac{(K_{IC})^2}{E}(1 - v^2) \tag{7}$$

where, E is the longitudinal modulus of elasticity and v is the Poisson's Ratio of the material.

3 EXPERIMENTAL INVESTIGATION

In this section, an experimental investigation of forces in the movement piston rods of the spillway floodgate of HPP Tucuruí is presented.

3.1 Experimental Procedure

The experimental test consisted of measuring forces in the piston rods of the spillway floodgate, shown in Fig. 2, making an opening of 2 m, followed by a total closure.

Figure 2. Movement Mechanism of the Floodgate

Choosing where to install the strain gages, as shown in Fig. 3, was based on Saint-Venant principle, which states that: "… stresses that may be produced in a body by applying, in a small part of its surface, a system of loads which is statically equivalent to zero, have inconsiderable magnitude in longer distances than the linear dimensions of the body.".

Due to lack of access to the notch of the piston rod, as observed in Fig. 3, and to the fact that stresses close to it are not uniform, the established criterion was installing strain gages at a distance greater than the diameter of the piston rod, starting from the notch. The uniformity of stresses where strain gages were installed, as well as the stresses at the notch of the piston rod where cracks occur, were part of the numerical investigation.

Figure 3. Strain Gages Installation

Specific steel strain gages were used, rosette ones at the top and unidirectional ones at the sides of the piston rod, installed as shown in Fig. 4. A data acquisition system, signal conditioners and specific cables for this type of operation were used.

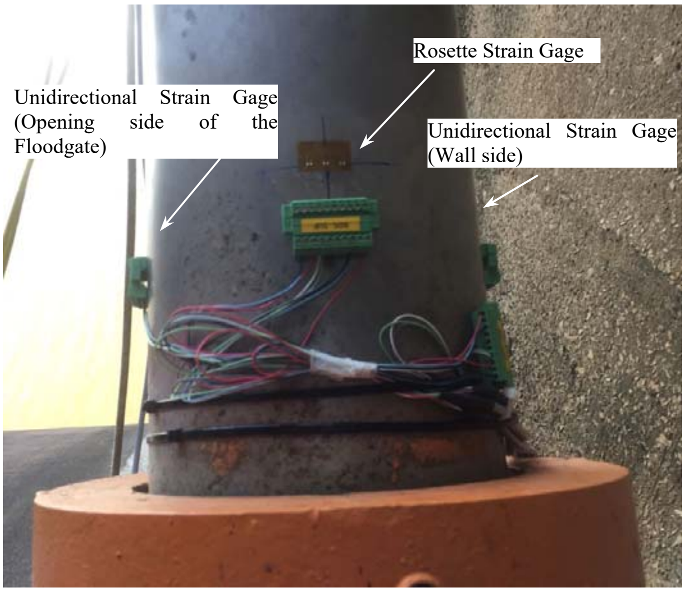

Figure 4. Top View of the Piston Rod

3.2 Experimental Results

The experimental results presented values in accordance with the original design calculation memory. It is observed in Fig. 5 that in the floodgate closure, a significant increase in stress occurred in piston rod Nº 37, which was not originally designed, measured by the rosette strain gage, installed at the top of the piston rod, as presented in Fig. 4.

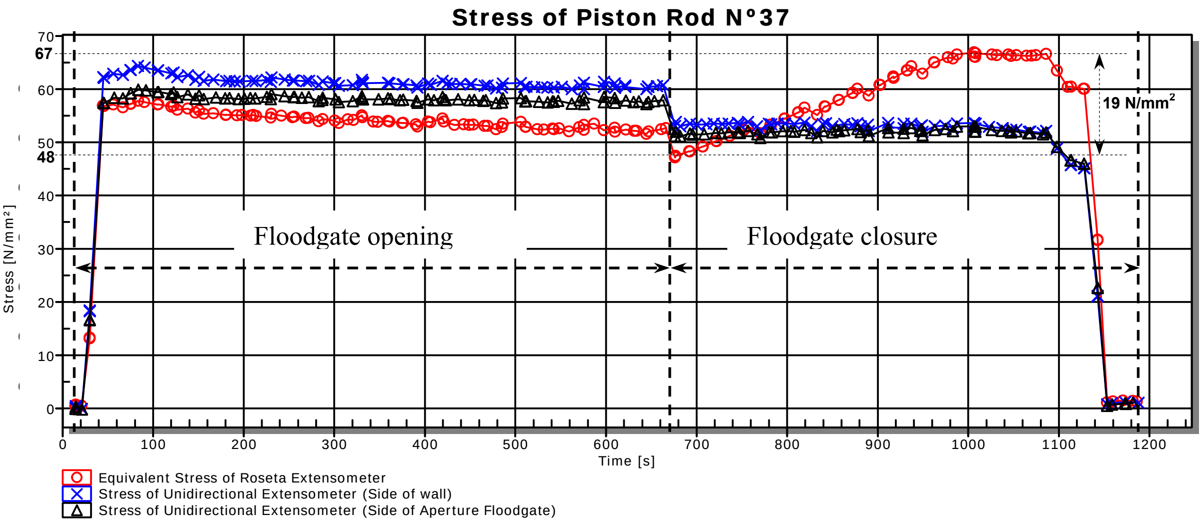

Figure 5. Stresses in Piston Rod Nº 37: Experimental Data

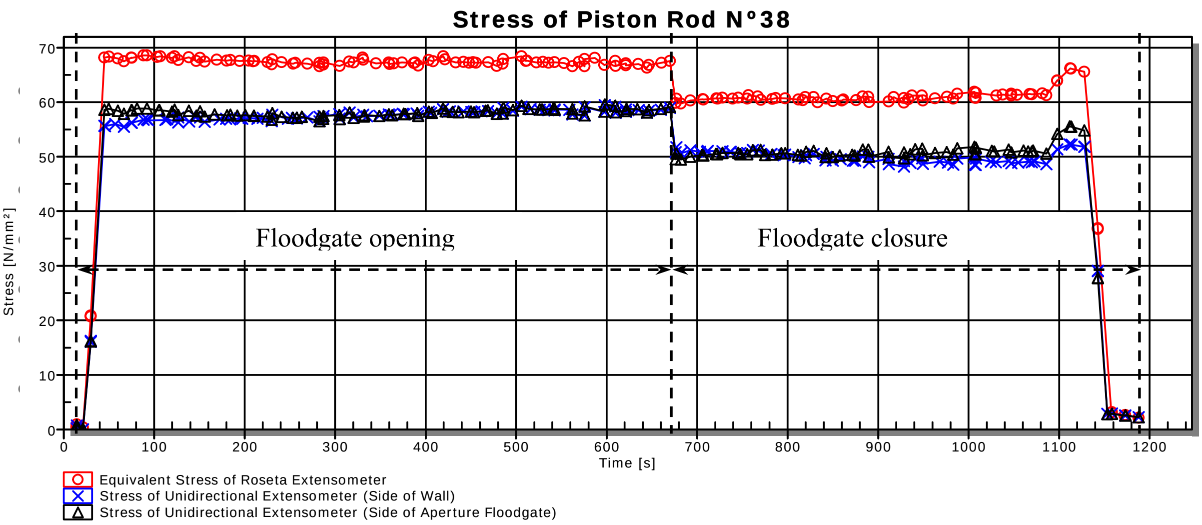

Figure 6. Stresses in Piston Rod Nº 38: Experimental Data

In Figure 7, the equivalente stress of the rosette strain gage of piston rod Nº 38 is observed, with a high sampling rate in a reduced time. In this Figure, the stress in the piston rod has variable amplitude and frequency, caused by the water flow through the floodgate.

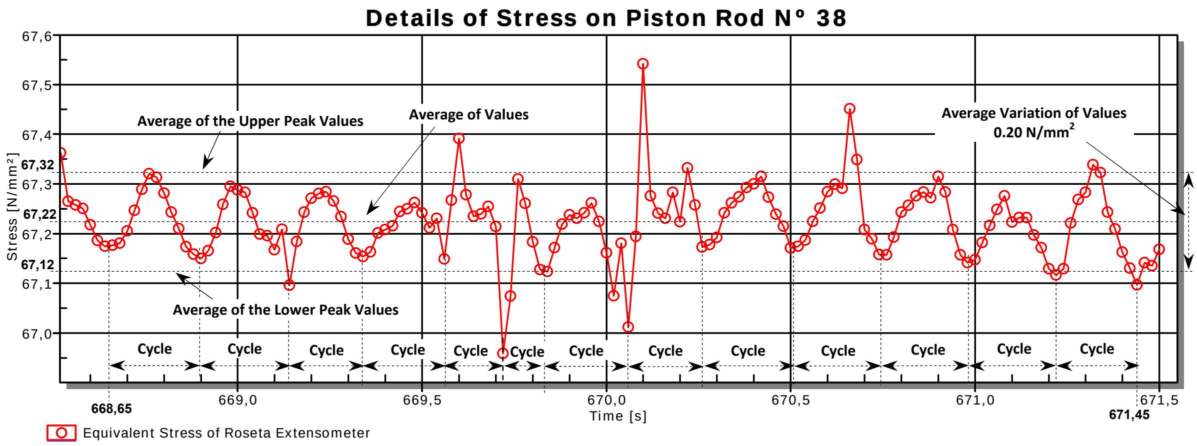

Figure 7. Stress Variation in Piston Rod Nº 38: Experimental Data

Experimental results used in the numerical analysis are presented in Fig. 7. The data sample was chosen because it presented amplitude and frequency values of the stress corresponding to when the floodgate had its greater opening during the test. In the simulation, data from piston rod Nº 38 were used, which showed no unforeseen design stresses.

In the experimental analysis, a mean tensile stress of 67.22 N/mm² (MPa) was verified at the section of the piston rod with diameter of 220 mm. It was also observed a mean variation of stress amplitude of 0.2 N/mm² (MPa) and a frequency of 4.64 Hz, equivalent to 13 cycles in 2.8 seconds.

4 NUMERICAL ANALYSIS

A numerical analysis was performed with a three-dimensional object, due to the need of entering geometric details such as notch, bevel and thread fillets, in order to obtain results close to the real situation. The commercial software ANSYS was used to generate the 3D object, automatic generation of finite element mesh and generation of stress, fatigue and fracture mechanics results.

4.1 Finite Element Modeling

The software was used to develop a geometrically correct finite element model, three-dimensional, representing the threaded end of the piston rod presented in Fig. 8. The constructive design is shown in Fig. 9 and the element mesh of the 3D object generated by the software is shown in Fig. 10.

Figure 8. Threaded End of the Piston Rod

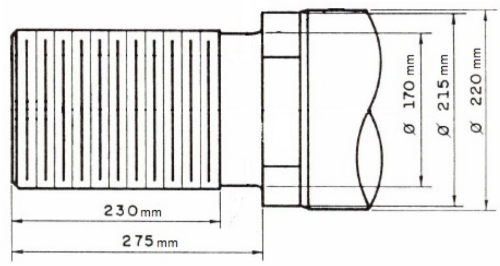

Figure 9. Constructive Design

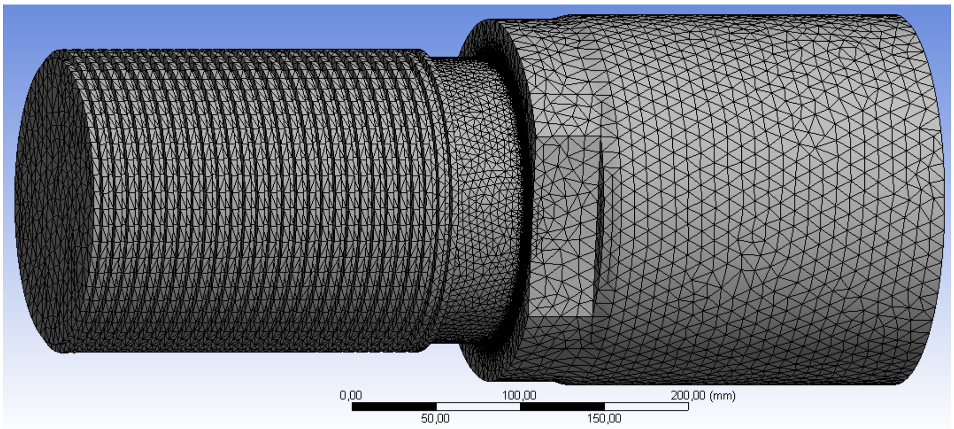

Figure 10. Finite Element Mesh of the 3D Object

A global mesh control was inserted in the whole object, with tetrahedral elements in order to reduce the mesh generation time. The main global mesh control parameters are presented in Table 4.

Table 4. Global Mesh Control Parameters

Parameter	Unit	Value
Min Size	mm	4.00
Max Face Size	mm	10.00
Max Tet Size	mm	30.00
Growth Rate	-	1.60

It was necessary to include a local mesh control in the notch of the piston rod, because its dimensions are close to the minimum size inserted in the global control and also because it is the interest point of analysis. The main local mesh control parameters are presented in Table 5.

Table 5. Local Mesh Control Parameters

Parameter	Unit	Value
Element Size	mm	0.50

The mesh generation software determined a value of 77% for the object mesh quality. This way, the great majority of mesh elements does not have strain. Fig. 10 presents a bar chart relating the quantity of mesh elements to the mesh quality.

4.2 Convergence Study

A tool from the software was used to automatically perform the mesh convergence study. A value of 5% was the maximum error between the maximum stresses of the solutions, with and without refinement. In Table 6, the stress values, stress percentage error, and number of nodes and elements of the convergence study are observed.

Table 6. Convergence Study Results

Solution	Maximum Stress (MPa)	Error (%)	Number of Nodes	Number of Elements
Without Refinement	410.60	-	362,719	241,364
With Refinement	412.32	0.42	1,044,974	719,359

4.3 Characteristics of the Material

The movement piston rods of the spillway floodgate are made of martensitic stainless steel, specified by ASTM A 276 as type 410 (or AISI 410) T-property. This property means that the steel is hardened by heat and other thermic treatments at a relative high temperature.

According to ASTM A 276, the AISI 410 T-property steel shall be in accordance with the requirements of: the chemical composition presented in Table 7; the mechanical testing presented in Table 8; and the stiffness, after thermic treatment, presented in Table 9.

Table 7. Chemical Requirements of AISI 410 steel

Type	C	Mn	P	S	Si	Cr	Ni	Mo	N	Others
410	Min: 0.08 Max: 0.15	Max: 0.04	Max: 0.04	Max: 0.03	Max: 1.00	Min: 11.15 Max: 13.5	…	…	…	…

Table 8. Mechanical Requirements of AISI 410 steel

Modulus of Elasticity (GPa)	Poisson's Ratio	Tensile Strength (MPa)	Yield Stress (MPa)	Elongation in 2 in. (%)	Area Reduction (%)
200	0.30	Min: 690	Min: 550	Min: 15	Min: 45

Table 9. Response to Thermic Treatment for AISI 410 steel

Type	Finish	Thermic Treatment Temperature (° C)	Quenchant	Hardness HRC
AISI 410	Hot	Min: 955	Air	Min: 35

4.4 Stress Concentration Study

In the analytical study of the stress concentration in the notch, Eq. (8) was used, taken from the book *Roark's Formulas for Stress and Strain* (Young and Budynas, 2002) for a square shoulder piece with fillet in circular shaft, as show in Fig. 11.

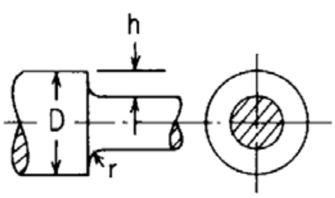

Figure 11. Square shoulder with fillet in circular shaft

$$\sigma_{max} = K_t \frac{4F_{nom}}{\pi(D-2h)^2} \quad (8)$$

where,

$$K_t = C_1 + C_2\left(\frac{2h}{D}\right) + C_3\left(\frac{2h}{D}\right)^2 + C_4\left(\frac{2h}{D}\right)^3 \quad (9)$$

$F_{nom} = Nominal\ Axial\ Force$

$D = Largest\ Diameter\ of\ the\ Axis$

$h = Notch\ Size$

$r = Notch\ Radius$

for $2.0 \leq h/r \leq 20.0$,

$$C_1 = 1.225 + 0.831\sqrt{h/r} - 0.010\, h/r \quad (10)$$

$$C_2 = -1.831 - 0.318\sqrt{h/r} - 0.049\, h/r \quad (11)$$

$$C_3 = 2.236 + 0.522\sqrt{h/r} - 0.176\, h/r \quad (12)$$

$$C_4 = -0.630 + 0.009\sqrt{h/r} - 0.117\, h/r \quad (13)$$

For a nominal force (F_{nom}) of 2,554.5 kN, largest diameter of the axis (D) of 220 mm, notch size (h) of 25 mm and notch radius (r) of 2 mm, the Factor of Stress Concentration (K_t) is 3.34 and the maximum stress in the notch (σ_{max}) is 375.5 MPa.

In the computational study of the stress at the notch of the piston rod, restrictions on the lateral areas of the thread fillets were inserted, simulating the support provided by the bottom fork clevis and a longitudinal force in the cross-sectional area of the piston rod, simulating the oil pressure on the piston of the hydraulic cylinder, as shown in Fig. 12.

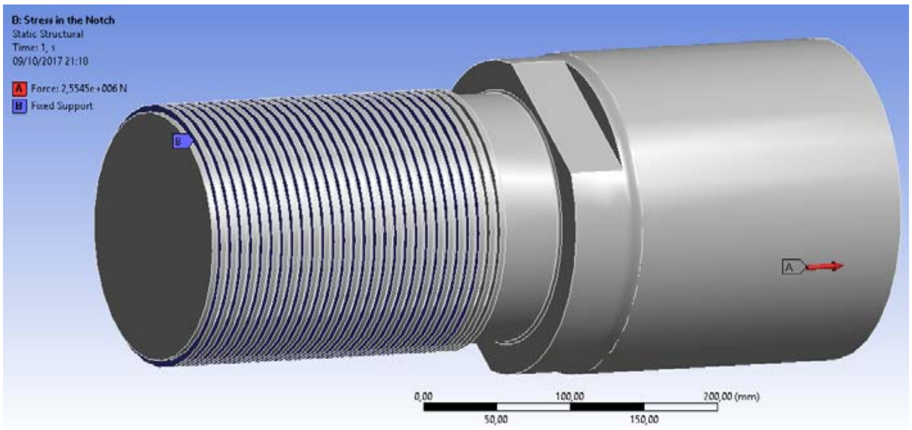

Figure 12. Support e Force

In Figure 13, there is the equivalent von Mises stress distribution, highlighting the highest stress value (412.32 MPa) located in the notch of the piston rod, the stress in the smallest diameter region (117.27 MPa) away from the notch of the piston rod, and the stress in the largest diameter region (67.27 MPa) close to where strain gages were installed for the experimental test.

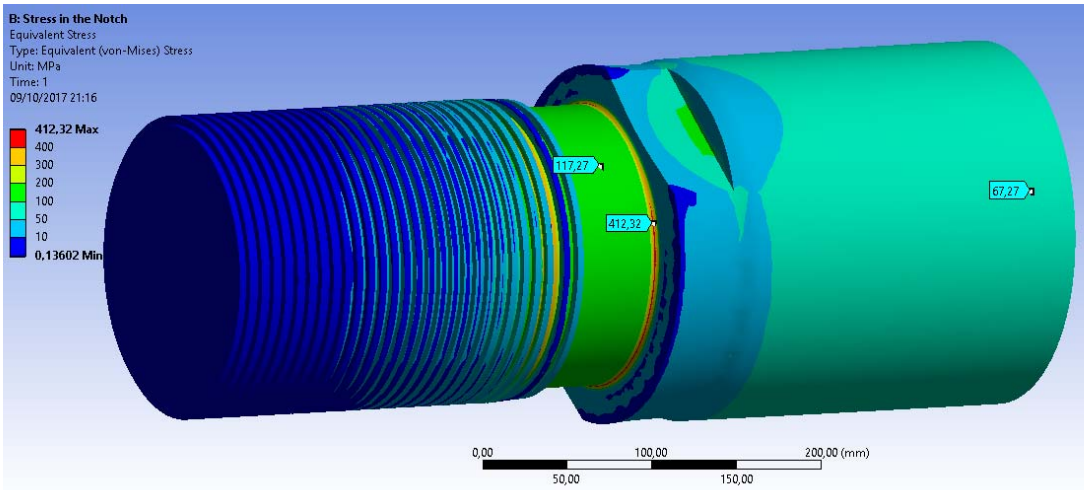

Figure 13. Equivalent von Mises Stresses in the Threaded End of the Piston Rod

In this computational study, a Stress Concentration Factor (K_t) of 3.52 was observed to be approaching the obtained value in the analytical study.

4.5 Fatigue Study

A fatigue study was performed considering as main factors of failure the values of maximum stress, stress variation and number of cycles from the experimental test. It is highlighted that other factors that influence the performance to fatigue, such as temperature and corrosion, were not considered.

A fatigue life study without using a Finite Element Analysis (FEA) was performed to obtain the approximate results. Eq. (3) and (4) were used with the parameters of the material in analysis and considering a variation of the nominal stress ($\Delta\sigma_{nom}$) of 3.50 MPa to obtain Eq. (14), aiming the calculation of the stress variation ($\Delta\sigma$).

$$(3.34x3.50)^2 = \Delta\sigma^2 + \frac{2x200{,}000}{(2x901)^{1/0.137}}\Delta\sigma^{(0.137+1)/0.137} \tag{14}$$

With a stress variation value ($\Delta\sigma$) of 11.68 MPa and using Eq. (2), a value of 2.92x10^{-5} for the total strain $\left(\frac{\Delta\varepsilon}{2}\right)$ was calculated, by Eq. (15).

$$\frac{\Delta\varepsilon}{2} = \frac{\Delta\sigma}{2x200{,}00} + \left(\frac{\Delta\sigma}{2x901}\right)^{1/0.137} \tag{15}$$

Finally, by Eq. (16), the number of reversals (2N) until failure was calculated.

$$\frac{\Delta\varepsilon}{2} = \frac{1035}{200{,}000}(2N)^{-0.09} + 0.45(2N)^{-0.59} \tag{16}$$

By the fatigue life study, without using FEA, a number of cycles (N) of about $4.8x10^{24}$ was obtained.

For checking the fatigue life through computational simulation, forces due to water flow through the floodgate, from the experimental test, were modeled as a sinusoid, with peak-to-peak amplitude of 0.2 MPa and a frequency of 4.64 Hz.

A fatigue resistance factor (k_f) of 0.82 was used to consider factors of surface finish, size, load type, temperature, reliability and fretting.

For mean stress correction, Smith-Watson-Topper (SWT) theory was used, because according to (Dowling, 2004), SWT equation for mean stress is a good choice for general use and has a simple equation of mean stress amplitude for all metals.

In Figure 14 is presented fatigue life, of the smallest diameter section of the piston rod caused by cyclic loads simulating the water flow through the floodgate adding to the nominal tensile strength of the piston rod caused by oil pressure on the piston. The figure highlights the result of fatigue life simulation at the critical point of the piston rod, where cracks and rupture occur ($1,83x10^{14}$ cycles).

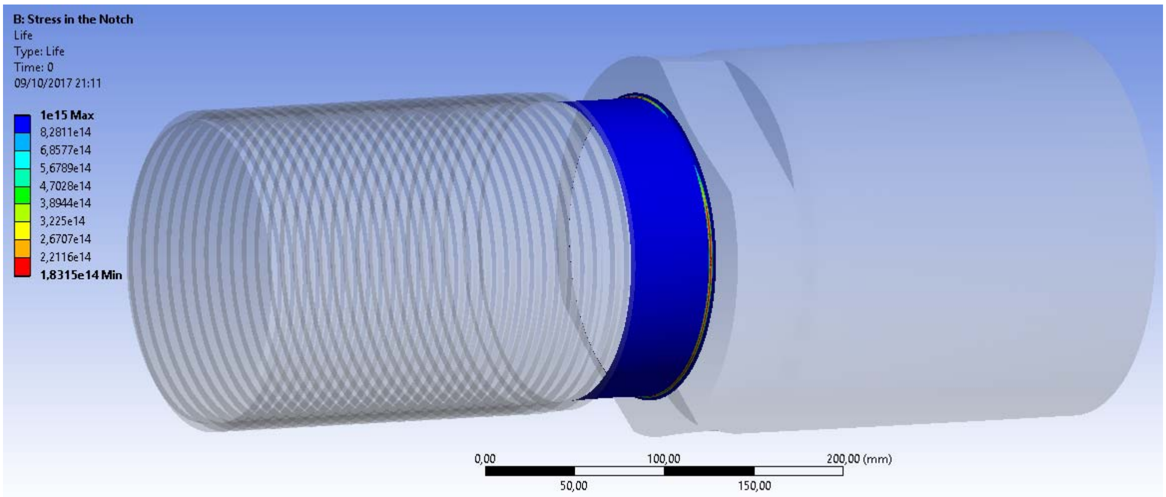

Figure 14. Distribution of Fatigue Life in the Smallest Diameter Section of the Piston Rod

4.6 Crack Study

In the crack study of the piston rod of the spillway floodgate, simulations of semi-elliptical cracks were performed, with different sets of parameters (size, depth). The results are presented in Table 10.

In the simulations, a semi-elliptical crack with a dominant hexahedral controled finite element mesh was inserted, in the region of the smallest diameter of the piston rod, as shown in Figs. 15 and 16.

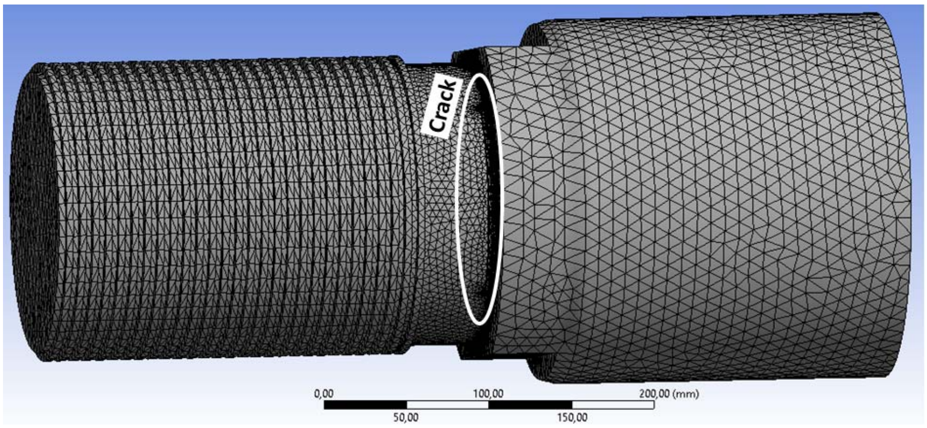

Figure 15. Finite Element Mesh of the 3D Object with Crack

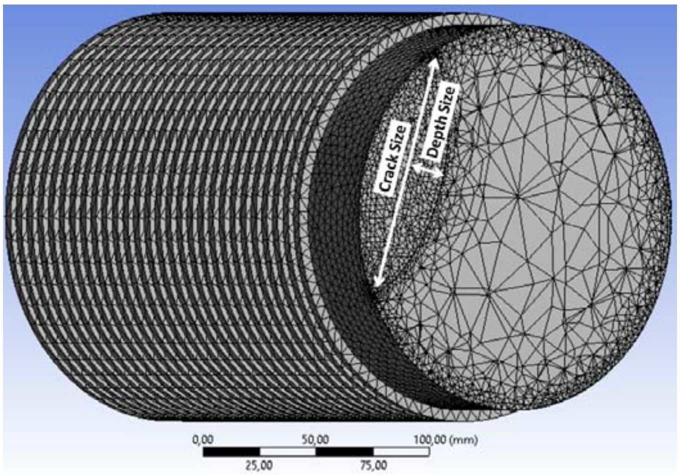

Figure 16. Detail of the Crack Mesh

A graphical view of the distribution of the *J integral* and von Mises stress at the end of the crack are presented in Figs. 17 and 18, respectively. These results refer to simulation #5.

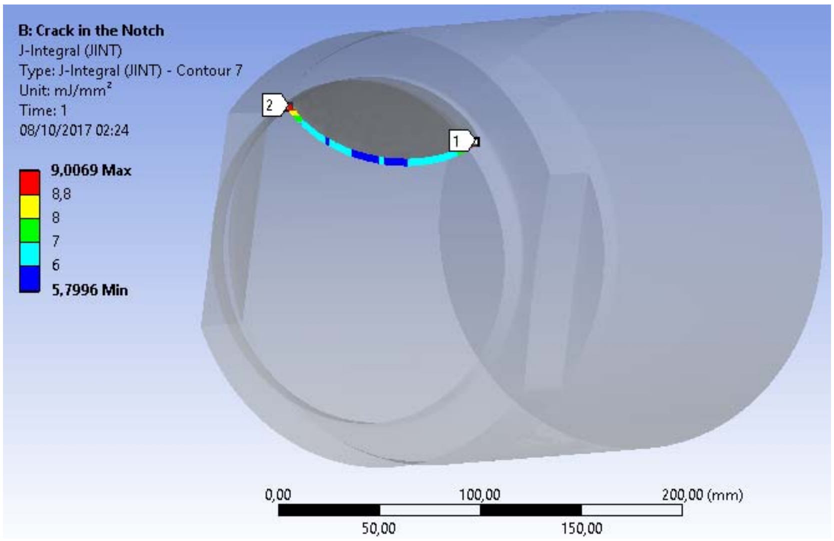

Figure 17. Distribution of the *J Integral* at the Crack in Simulation #5

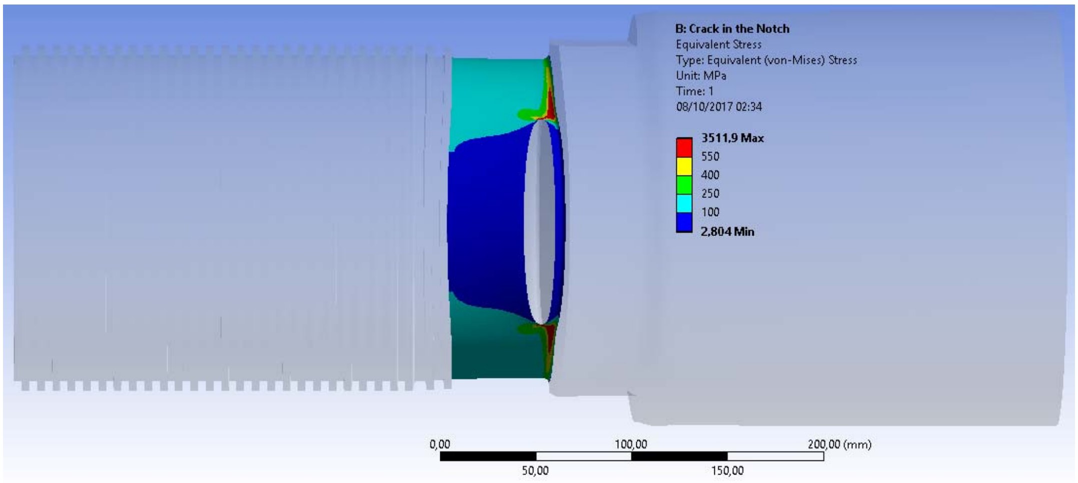

Figure 18. Distribution of the von Mises Stress Crack of the Simulation #5

Table 10. Results of Crack Simulations

Simulation	Crack Size (mm)	Crack Depth (mm)	von Mises Maximum Stress (MPa)	Maximum Stress Intensity Factor (MPa$\sqrt{mm}$)	Maximum *J Integral* (mJ/mm^2)
#1	14,00	1,25	559,91	428,58	0,84
#2	75,00	30,00	4.048,80	1.407,60	9,85
#3	90,00	25,00	3.872,60	1.411,80	9,71
#4	100,00	20,00	3.657,60	1.399,80	9,25
#5	107,00	17,50	3.511,90	1.394,30	9,01

5 ANALYSIS OF THE RESULTS

Results obtained in the experimental test presented nominal stress values in accordance with design values. A stress increase in piston rod Nº 38 is highlighted, unforeseen in design, probably due to lack of lubrification at the bottom fork clevis bearing. This resistance to rotation movement of the bottom fork clevis was only detected by the rosette strain gage at the top of the piston rod, meaning flexure existance.

The variable load of the piston rod, caused by water flow through the floodgate, has low values of frequency and stress amplitude variation, making the modeling of this load not fundamental for fatigue analysis. Performing a more conservative modeling or even using the data set from the experimental test as load, the results for fatigue life will be close to this study's ones.

In all simulations, finite element meshes presented coherent results, specially in the smallest diameter region of the piston rod. It is worth highliting the importance of using hexahedral elements to truly represent the stress field in the crack, whose gradient is naturally high. The convergence study was satisfactory and the mathematical model did not present singularities.

The maximum values of stress concentration in the notch of the piston rod have a higher stress concentration factor than the one from some formulas, tables and abacuses. It is highlighted that the finite element mesh was refined enough to ensure stresses were close to the real situation and to represent the gradient of stresses correctly.

Fatigue studies, as expected, presented results of crack initiation in the region of highest stress concentration. Due to the reduced stress variation amplitude caused by water flow through the floodgate, about 0.3% of the nominal stress, the necessary number of cycles to cause crack initiation in this type of steel is very high, so that the number of cycles in days and with a frequency of 4.64 Hz, result in a longer lifespan for the piston rod than the dam's one. The difference of values obtained in the analytical and computational study is due to using the fatigue resistance factor (k_f) and the mean stress correction theory (SWT). It is recommended that the ε-N curve parameters be measured in laboratory tests, even with changes of these parameters, the same conclusion above will be obtained.

In the crack studies, it was observed that size and depth of the semi-elliptical crack are geometric characteristics that determine if there will be rupture in the piston rod, because they influence the values of stress intensity factor and the *J integral*. It was observed that, increasing the crack size, the depth that causes the rupture of the piston rod decreases. As presented in simulation #1 of Table 10, cracks with depths greater than 3 mm cause stresses that create a plastification zone in the region close to the end of the crack.

6 CONCLUSION

An experimental and numerical investigation about the cause of the fracture of the piston rod of the spillway floodgate of HPP Tucuruí was presented in this paper.

The fatigue study showed that crack initiation in the entire piston rod of the spillway of HPP Tucuruí, exclusively due to cyclic forces caused by the water flow through the floodgate, is unlikely. Other factors must be involved for crack initiation due to fatigue, such as corrosion and friction at the bottom fork clevis bearing.

The piston rod ruptures when the crack reaches about 17.5-30 mm of depth. However, any found crack must be a reason for considering replacement of the piston rod, because once it is initiated, the crack propagates easily, being hard to monitor its growth. Liquid penetrant testing in all working piston rods is extremely recommended to identify cracked piston rods and then replace them.

A crack propagation study shall be performed, to compare the operation time of fractured piston rods with the crack propagation time to a size that reaches the critical value of tenacity to fracture. It will also be performed a metallographic replic test on two spare piston rods from the same design and lot, that have never been used. This test will check, in a small sample space, if there are surface cracks in the smallest diameter region of the piston rod, from the manufacturing process.

To conclude the cause of the rupture in the piston rod, it will be necessary to perform tensile, fatigue, charpy-V and accelerated corrosion tests, as well as chemical, fractographic and metallographic analysis of the fractured parts. Problems in the manufacturing process, mainly related to the thermic treatment of the material, may be the cause of the piston rod rupture. This investigation is being continued and will be presented after laboratory tests, in future studies.

ACKNOWLEDGMENTS

The AUTHORS generously thank Centrais Elétricas do Norte do Brasil S/A and Federal Univeristy of Pará for all technical and financial support given to this research project.

REFERENCES

[1] Melo, R. O., Severo, D. S. Pohlmann, J. R. Análise por Elementos Finitos na Resolução de Problemas Crônicos em Estruturas – Caso do Descarregador de Navios da ALUMAR. Abraman, 2005.

[2] Chaves, A. P., 2010. *Estudo Comparativo da Vida em Fadiga de Aços Fundidos e Forjados de Alta Resistência para Utilização em Acessórios de Linhas de Ancoragem de Plataformas Offshore*. Dissertação de Mestrado, CEFET/RJ.

[3] Meggiolaro, M. A., Castro, J. T. P., 2002. Avaliação das Estimativas dos Parâmetros SN e εN no Projeto à Fadiga. In *II National Congress of Mechanical Engineering*, João Pessoa, Paraíba.

[4] Meggiolaro, M. A., Castro, J. T. P, 2004. *Statistical Evaluation of Strain Life Fatigue Crack Initiation Predictions*. *International Journal of Fatigue* v.26, p.463-476.

[5] Dowling, N., 2004. *Mean Stress Effects in Stress-Life and Strain-Life Fatigue*, SAE Technical Paper 2004-01-2227.

[6] Chiodo, M. S. G., 2009. *Procedimento de Avaliação da Integral J e CTDO para Dutos com Trincas Circunferenciais Submetidas à Flexão e Aplicações à Instalação de Risers pelo Método Carretel*. Dissertação de Mestrado, USP/SP.

[7] Hise, A. L., 1987. *Fracture Toughness Characterization of Type 410 Stainless Steel*, Electric Power Research Institute.

[8] Srinivasan, M., Seetharamu, S., 2012. *Fracture Toughness of Metal Castings*, Science and Technology of Casting Processes.

[9] Young, W. C., Budynas R. G., 2002. *Roark's Formulas for Stress and Strain*. 7 ed. New York: McGraw Hill.